

Photolithography Process Simulation for Integrated Circuits and Microelectromechanical System Fabrication *

Zhou Zaifa[†], Huang Qing'an, and Li Weihua

(Key Laboratory of MEMS of the Ministry of Education, Southeast University, Nanjing 210096, China)

Abstract: Simulations of photoresist etching, aerial image, exposure, and post-bake processes are integrated to obtain a photolithography process simulation for microelectromechanical system (MEMS) and integrated circuit (IC) fabrication based on three-dimensional (3D) cellular automata (CA). The simulation results agree well with available experimental results. This indicates that the 3D dynamic CA model for the photoresist etching simulation and the 3D CA model for the post-bake simulation could be useful for the monolithic simulation of various lithography processes. This is determined to be useful for the device-sized fabrication process simulation of IC and MEMS.

Key words: cellular automata; process simulation; photolithography simulation; model; TCAD

EEACC: 2570; 2560; 2550E

CLC number: TN4

Document code: A

Article ID: 0253-4177(2006)04-0705-07

1 Introduction

As the dimensions of integrated circuits (IC) are scaling down to the nanometer regime and the complexity of micro-electro-mechanical system (MEMS) design and fabrication is increasing, three-dimensional (3D) photolithography simulation has become necessary for accurate analysis of complex structures such as contacts, corners, islands, and 3D defects^[1]. Simulation aids in understanding the effects of parameters during photolithography so that masks can be optimized and the accuracy of critical structures and the reliability of devices can therefore be improved^[2]. The simulation of photolithography is a complex task that usually includes precise modeling in aerial image simulation, exposure simulation, post-bake simulation, and photoresist etching simulation (development simulation)^[3]. The etching simulation is usually the most time-consuming step and greatly affects the accuracy of the whole photolithography simulation. So a fast and accurate 3D model for photoresist etching is greatly desired for effective photolithography process simulation.

Due to its advantages such as ease in handling topological changes, adaptive mesh methods, and

the simplest models for implementation in MEMS and IC fabrication process simulation, the cellular automata model, which was first presented by von Neumann following Ulam's suggestions^[4], has been successfully applied to the simulation of various fabrication processes such as photoresist etching^[5-7], deposition^[8,9], and silicon anisotropic etching^[10]. The 3D dynamical CA model for photoresist etching simulation^[11], which is extended from the 2D dynamical CA model^[5], has been presented and tested using well-known etching rate distribution functions and is demonstrated to be accurate, fast and stable.

In this paper, simulations of the photoresist etching process using the 3D dynamic CA model and the post-bake process using the 3D CA model are integrated together for the first time with an aerial image simulation and an exposure process simulation to accurately describe the effects of parameters during the photolithography process. The simulation results agree well with available experimental results. This indicates that the 3D dynamic CA model for photoresist etching simulation and 3D CA model for post-bake simulation are accurate, fast, and can be integrated with other photolithography simulation steps. This will be useful for the simulation of the device-sized fabrication

* Project supported by the National Outstanding Young Scientists Foundation of China (No. 50325519)

[†] Corresponding author. Email: zhouzaifa@yahoo.com.cn

Received 17 January 2006, revised manuscript received 15 February 2006

process of IC and MEMS.

2 3D dynamical CA model

The photoresist is divided into $l \times m \times n$ identical cubic cells with side length a , and the 3D Moore neighborhood is adopted in the 3D dynamic CA model, as shown in Fig. 1. There are 6 adjacent cubic cells, 12 diagonal cubic cells, and 8 point cubic cells in the neighborhood of cell (i, j, k) . A boundary cell between the internal photoresist and etchant will be etched by etchant flowing from its

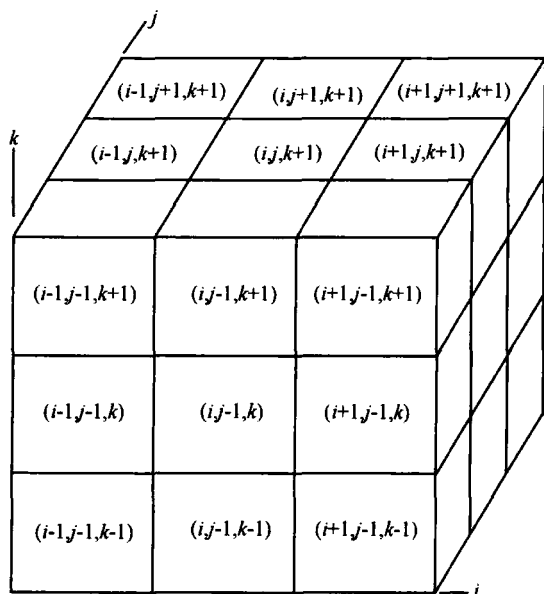


Fig. 1 Moore neighborhood of the cellular automata

neighbors. Theoretically, the effect of etchant from all neighbors should be taken into account when the state of cell (i, j, k) is updated. But the 8 point diagonal cells do not significantly affect the change of the state of cell (i, j, k) . So the effect of the point diagonal cells is neglected in this model. The local state $C_{i,j,k}(t)$ of each cell at time t is defined as the ratio of the etched volume $V_e(t)$ to the total volume V_c :

$$C_{i,j,k}(t) = \frac{V_e(t)}{V_c} \quad (1)$$

The update rule is then given by Ref. [11]:

$$C_{i,j,k}(t_1 + T) = C_{i,j,k}(t_1) + \frac{V_e(t_1 + T)_{\text{adjacent}} + V_e(t_1 + T)_{\text{diagonal}}}{a^3} \quad (2)$$

$$V_e(t_1 + T)_{\text{adjacent}} = (a - d_{ih} - d_{il}) \times (d_{jl}d_{kl} + d_{jl}d_{kh} + d_{jh}d_{kl} + d_{jh}d_{kh}) +$$

$$(a - d_{yh} - d_{yl})(d_{il}d_{kl} + d_{il}d_{kh} + d_{ih}d_{kl} + d_{ih}d_{kh}) + (a - d_{kh} - d_{kl})(d_{il}d_{jl} + d_{il}d_{jh} + d_{ih}d_{jl} + d_{ih}d_{jh}) + (a - d_{ih} - d_{il})(a - d_{kl} - d_{kh})(d_{jl} + d_{jh}) + (a - d_{jh} - d_{jl})(a - d_{kl} - d_{kh})(d_{il} + d_{ih}) + (a - d_{kh} - d_{kl})(a - d_{jl} - d_{jh})(d_{il} + d_{ih}) + d_{il}d_{jl}d_{kl} + d_{il}d_{jl}d_{kh} + d_{il}d_{jh}d_{kl} + d_{il}d_{jh}d_{kh} + d_{ih}d_{jl}d_{kl} + d_{ih}d_{jl}d_{kh} + d_{ih}d_{jh}d_{kl} + d_{ih}d_{jh}d_{kh} \quad (3)$$

$$V_e(t_1 + T)_{\text{diagonal}} = \frac{D}{2} R_{i,j,k}^2 (T + Tc_{i+1,j,k+1}(t_1))^2 + \frac{D}{2} R_{i,j,k}^2 (T + Tc_{i+1,j,k-1}(t_1))^2 + \frac{D}{2} R_{i,j,k}^2 (T + Tc_{i-1,j,k+1}(t_1))^2 + \frac{D}{2} R_{i,j,k}^2 (T + Tc_{i-1,j,k-1}(t_1))^2 + \frac{D}{2} R_{i,j,k}^2 (T + Tc_{i,j+1,k+1}(t_1))^2 + \frac{D}{2} R_{i,j,k}^2 (T + Tc_{i,j+1,k-1}(t_1))^2 + \frac{D}{2} R_{i,j,k}^2 (T + Tc_{i,j-1,k+1}(t_1))^2 + \frac{D}{2} R_{i,j,k}^2 (T + Tc_{i,j-1,k-1}(t_1))^2 + \frac{D}{2} R_{i,j,k}^2 (T + Tc_{i+1,j+1,k}(t_1))^2 + \frac{D}{2} R_{i,j,k}^2 (T + Tc_{i+1,j-1,k}(t_1))^2 + \frac{D}{2} R_{i,j,k}^2 (T + Tc_{i-1,j+1,k}(t_1))^2 + \frac{D}{2} R_{i,j,k}^2 (T + Tc_{i-1,j-1,k}(t_1))^2 \quad (4)$$

where $V_e(t_1 + T)_{\text{adjacent}}$ and $V_e(t_1 + T)_{\text{diagonal}}$ describe the effects from the adjacent and the diagonal cells, respectively. $Tc(t_1)$ is the time compensation value. The parameter D is adopted to describe the effect of the diagonal cells, and different values will be used according to the state of the diagonal cells and the state of the shared adjacent cells of these diagonal cells and cell (i, j, k) . The variables in Eq. (3) are defined as

$$\begin{cases} d_{il} = R_{i,j,k}(T + Tc_{i-1,j,k}(t_1)) \\ d_{ih} = R_{i,j,k}(T + Tc_{i+1,j,k}(t_1)) \\ d_{jl} = R_{i,j,k}(T + Tc_{i,j-1,k}(t_1)) \\ d_{jh} = R_{i,j,k}(T + Tc_{i,j+1,k}(t_1)) \\ d_{kl} = R_{i,j,k}(T + Tc_{i,j,k-1}(t_1)) \\ d_{kh} = R_{i,j,k}(T + Tc_{i,j,k+1}(t_1)) \end{cases} \quad (5)$$

In the 3D dynamic CA model, only the boundary cells are processed, and an interior cell that has at least one fully etched adjacent or diagonal neighbor becomes a boundary cell. At the beginning of the simulation, the photoresist is divided into $l \times m$

$\times n$ cubic cells ,and all the cells are in the “ 0 ” state (unetched) ,and the time compensation value for all cells is “ 0 ”. Initial conditions are imposed by changing the states of some cells ,and the etching process starts along the etch boundary cells. Some boundary cells will gradually become fully etched , and those fully etched cells will be excluded from the boundary cell array during the simulation. At the same time , some interior cells will become boundary cells according to the CA rules. These new boundary cells will be inserted into the boundary cell array ,and pointers corresponding to these new boundary cells are also created. Considering that there is always a trade-off between simulation accuracy and speed —namely, a large time step will reduce the simulation accuracy, whereas a small time step will reduce the simulation

speed —the time step value in the 3D dynamic CA model of $T = a/10R_{max}$ is adopted ,where R_{max} is the maximum etch rate of the cells.

The model has been tested using the well-known etching rate distribution functions and has been found to be stable ,fast ,and accurate^[4]. The $1.0\mu\text{m} \times 1.0\mu\text{m} \times 1.0\mu\text{m}$ photoresist was divided into $100 \times 100 \times 100$ identical cubic cells ,and the test function is given by^[12]

$$R_{(x,y,z)} = 4x^2\mu\text{m/s} \tag{6}$$

where x and y are the distances on the wafer ,and z is the depth of the photoresist. The 3D simulation profiles corresponding to different etching time steps are shown in Figs.2(a) and (b). The simulation time was found to be 35.9s on a Sun Ultra work station.

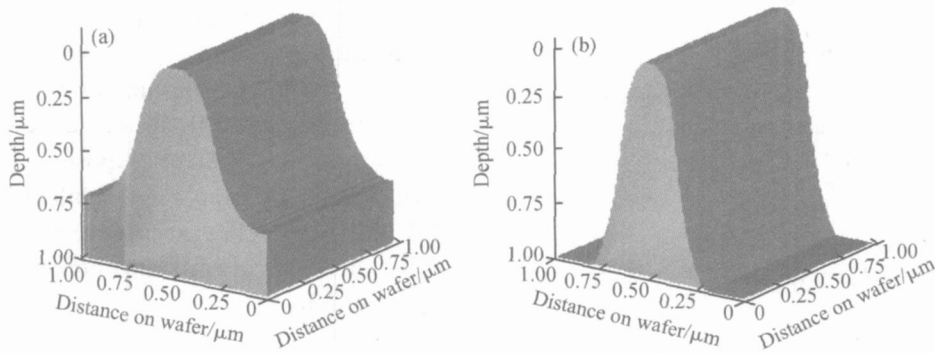


Fig. 2 Simulation profiles with Equation(6) (a) and (b) correspond to different etching times.

The 3D dynamic CA model for the simulation of photoresist etching has been found to be accurate ,fast ,and stable ,but it is necessary to integrate simulations of aerial image ,exposure ,post-bake , and photoresist etching in order to accurately describe the effects of parameters during the photolithography process. In the following section , the photoresist etching simulation using the 3D dynamic CA model will be integrated with simulations of the aerial image ,exposure process , and post-bake process.

3 Simulation and discussion

The general steps for photolithography simulation are aerial image simulation ,exposure simulation ,post-bake simulation ,and photoresist etching simulation. The aerial image exposure pand and and and and and image distribution on the re-

sist-coated wafer. The exposure process generates acid in the resist. During the subsequent post-bake process , the resist undergoes an acid-catalyzed cross-linking reaction which determines the etch rate distribution in the photoresist. In the last step ,the photoresist is etched according to the etch rate distribution obtained from the two former simulation steps. The typical simulation steps for the photolithography process of chemical amplification photoresists are shown in Fig. 3.

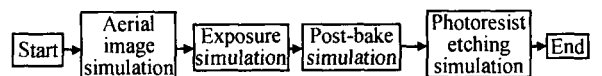


Fig. 3 Typical simulation steps for photolithography process of chemical amplification photoresists

The new SPLAT^[13] can efficiently express the influence of various parameters of the image tool for high numerical aperture (NA) lithography resists (NA > 0.6). With the parameters listed in Ta-

ble 1 ,such as partial coherence ,focus ,and exposure dose I ,the new SPLAT is successfully employed to simulate the aerial image on the resist-coated wafer ,and bottom anti-reflective coating (BARC) technology is implemented using AR3 anti-reflectant . Then the well-known Dill 's

Table 1 Parameters for hard-contact exposure process of UVTM113 chemical amplification photoresist

| Simulation step | Parameters | Reference |
|-----------------------------|---|-----------|
| Aerial image | $n_{\text{silicon}} = 1.577, n_{\text{resist}} = 1.786,$ $k_{\text{silicon}} = -3.588, n_{\text{AR3}} = 1.46,$ $k_{\text{AR3}} = -0.47, \text{focus} = 0,$ $I = 13 \text{ mJ/cm}^2, \text{KrF},$ $\text{NA} = 0.63, \sigma = 0.6$ | [13,15] |
| Exposure | Dill A = $0.0746 \mu\text{m}^{-1},$ Dill B = $0.5636 \mu\text{m}^{-1},$ Dill C = $0.0411 \text{ cm}^2/\text{mJ},$ [PAG] ₀ = 1 | [15,16] |
| Post-bake | Time = 90s, Temperature = 125 °C, $k_1 = 0.7068 \text{ s}^{-1},$ $k_2 = 0.0001 \text{ s}^{-1},$ $p = 1, r = 1, q = 1.34,$ [B] = 0.264, $M_0 = 1$ | [15~17] |
| Photoresist etch simulation | $N = 1.345, R_{\text{max}} = 0.8944 \mu\text{m/s},$ $R_{\text{min}} = 5.8 \times 10^{-5} \mu\text{m/s},$ $n_{\text{notch}} = 22.367,$ $M_{\text{th,notch}} = 0.586, \text{Time} = 45\text{s},$ Temperature = 20 | [18] |

ABC model^[14], which was first presented to model the exposure process of diazo-type resists, is employed to model the exposure process of chemically amplified photoresists. Dill 's ABC model is used to describe the reaction during the exposure process as

$$\frac{\partial [\text{PAG}]}{\partial t} = -C_{\text{Dill}} I [\text{PAG}] \quad (7)$$

$$= A_{\text{Dill}} [\text{PAG}] + B_{\text{Dill}} \quad (8)$$

where $A_{\text{Dill}} (\mu\text{m}^{-1}), B_{\text{Dill}} (\mu\text{m}^{-1}),$ and $C_{\text{Dill}} (\text{cm}^2/\text{mJ})$ are the parameters of Dill 's ABC model, [PAG] is a normalized concentration of photoacid generator, and I is the exposure illumination power density obtained from the aerial image simulation. Equations (7) and (8) are used to calculate parameter [A] and the normalized acid generated. After the

exposure is calculated, the normalized acid generated is $[A](0) = 1 - [\text{PAG}]$, which will be used as the initial condition for the following post-bake simulation.

The exact changes and mechanism during the post-bake process are complex, but a relatively simple theory is presented to explain the reaction mechanism^[15]. According to this theory, the reaction occurring in the photoresist cells can be described by a cellular automata model given by

$$m_{i,j,k}(t) = m_{i,j}(t-T) - k_1 [A]_{i,j,k}^q(t-T) \times m_{i,j,k}(t-T) \times T \quad (9)$$

$$[A]_{i,j,k}(t) = [A]_{i,j,k}(t-T) - k_2 [A]_{i,j,k}(t-T) \times T \quad (10)$$

where T is the time step in the post-bake simulation, $[A]_{i,j,k}(t)$ is the normalized acid generated in cell (i, j, k) at time t , and the initial value of $[A]_{i,j,k}(t)$ is $[A]_{i,j,k}(0)$. Also, $m_{i,j,k}(t)$ is the normalized inhibitor concentration in cell (i, j, k) at time t , k_1 and k_2 are the reaction rate coefficients, and q is a parameter related to the type of photoresist. The final normalized inhibitor concentration $m_{i,j,k}$ after exposure simulation and post-bake simulation can be calculated using Eqs. (9) and (10). Thus, according to the notch model^[16], the etch rate for all photoresist cells can be calculated by

$$R(m_{i,j,k}) = R_{\text{max}} (1 - m_{i,j,k})^n \times \frac{(a+1)(1 - m_{i,j,k})^{n_{\text{notch}}}}{a + (1 - m_{i,j,k})^{n_{\text{notch}}}} + R_{\text{min}} \quad (11)$$

$$a = \frac{(n_{\text{notch}} + 1)}{(n_{\text{notch}} - 1)} (1 - M_{\text{th,notch}})^{n_{\text{notch}}} \quad (12)$$

where R_{max} is the maximum etch rate of the photoresist, R_{min} is the minimum etch rate of the photoresist, n is the sensitivity of the developer, n_{notch} is the sensitivity of the notch, $M_{\text{th,notch}}$ is the threshold inhibitor concentration where the notch occurs, and $m_{i,j,k}$ is the final normalized inhibitor concentration in cell (i, j, k) .

According to the available parameter values of UVTM113 chemical amplification photoresist^[16~18], as listed in Table 1, the etch rate for all photoresist cells can be determined so that the 3D dynamic CA model can be employed to accomplish photoresist etching simulation. Thus the whole photolithography of UVTM113 chemical amplification photoresist can be successfully simulated.

Figures 4 and 5 show the simulation profiles of photolithography of UVTM113 photoresist corresponding to two different mask shapes. Figures 4

(a) and (b) are 3D views of the simulation results corresponding to different time steps. The etching times are 22s and 45s for Figs. 4 (a) and (b), respectively. Figures 4(c) and (d) are cross-sectional views of the simulation and corresponding experimental results^[18]. Figures 5 (a) and (b) show

cross-sectional views of the simulation and the corresponding experimental results^[18] for 110nm/220nm line/ space with a different focus value of -0.2. The etching time in Fig. 5 is 45s. The above simulation results agree well with available experimental results.

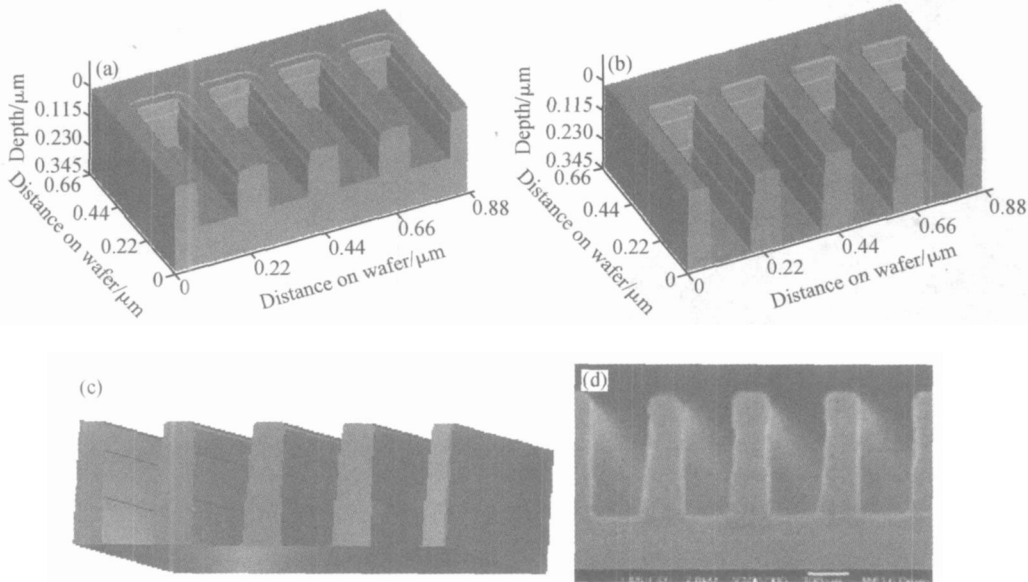


Fig. 4 Simulation profiles of photolithography process for UVTM 113 chemical amplification photoresist (a), (b) 3D view of the simulation results corresponding to 22s and 45s; (c), (d) Cross-section view of simulation and corresponding experimental results^[18]

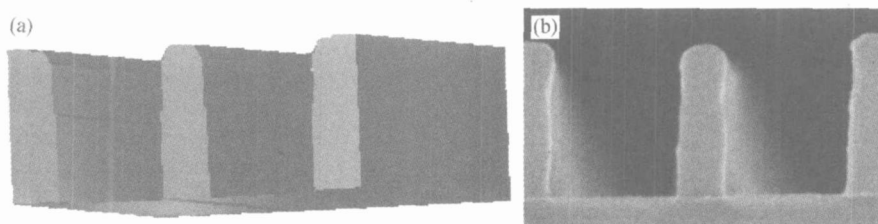


Fig. 5 Cross-section view of simulation (a) and corresponding experimental (b) results^[18] for 110nm/220nm line/space with a different focus value of -0.2

Figure 6 shows the photolithography simulation results for capacitor fabrication, which also agrees with available experimental results^[3,71]. The results indicate that the photoresist etching simulation using the 3D dynamic CA model can be successfully integrated with other photolithography simulation steps, so that the effect of parameters during the photolithography process can be accurately described.

Although only the photolithography process of UVTM 113 chemical amplification photoresist is simulated in this paper, since the aerial image, exposure, post-bake, and photoresist etching simulations are relatively independent, the 3D dynamic CA model for the simulation of photoresist etching and 3D CA model for the simulation of post-bake can also efficiently simulate the photolithography process of other photoresists.

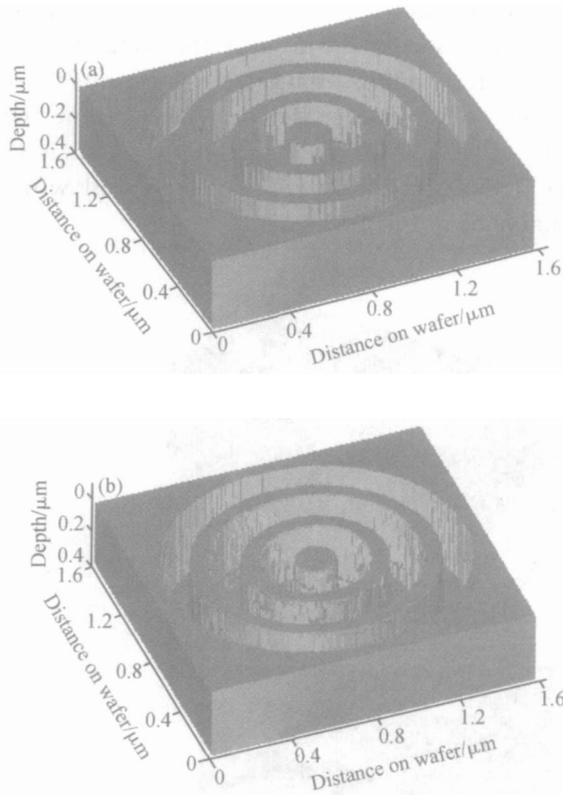


Fig. 6 Photoresist etching profiles for capacitor fabrication (a) and (b) correspond to different etching times.

4 Conclusion

The photoresist etching simulation using the 3D dynamic CA model and post-bake simulation using the 3D CA model have been successfully integrated with aerial image simulation and exposure process simulation for UVTM 113 chemical amplification photoresist. The simulation results agree well with available experimental results, indicating that the 3D dynamic CA model for photoresist etching simulation and 3D CA model for post-bake simulation are accurate, fast, and can be integrated with other photolithography simulation steps. This will be useful for the device-sized fabrication process simulation of IC and MEMS.

References

- [1] Strojwas A J, Zhu Zhengrong, Ciplickas D, et al. Layout manufacturability analysis using rigorous 3-D topography simulation. IEEE International Semiconductor Manufacturing Symposium, 2001 :263
- [2] Cole D C, Barouch E, Conrad E D, et al. Using advanced simulation to aid microlithography development. Proceedings of the IEEE, 2001, 89(8) :1194
- [3] Karafyllidis I. A three-dimensional photoresist etching simulator for TCAD. Modeling and Simulation in Materials Science and Engineering, 1999, 7(2) :157
- [4] Neumann J. Theory of self-reproducing automata. Urbana :University of Illinois Press, 1966
- [5] Zhou Zaifa, Huang Qing'an, Li Weihua, et al. A novel 2-D dynamic cellular automata model for photoresist etching process simulation. Journal of Micromechanics and Microengineering, 2005, 15(3) :652
- [6] Zhou Zaifa, Huang Qing'an, Li Weihua, et al. Negative chemical amplification process simulation in integrated circuits and microelectromechanical systems fabrication. ICO-20, 2005
- [7] Strasser E, Selberherr S. Algorithms and models for cellular based topography simulation. IEEE Trans Computer-Aided Design Integrated Circuit Systems, 1995, 14(5) :1104
- [8] Karafyllidis I, Georgoulas N, Hagouel P I, et al. Simulation of deposition-topography granular distortion for TCAD. Modeling and Simulation in Materials Science and Engineering, 1998, 6(2) :199
- [9] Huang Qing'an, Zhou Zaifa, Li Weihua, et al. A modified cellular automata algorithm for boundary movement of deposition topography simulation. Journal of Micromechanics and Microengineering, 2006, 16(1) :1
- [10] Jiang Yanfeng, Huang Qing'an. Simulation of silicon anisotropic etching using cellular automata method. Chinese Journal of Semiconductors, 2005, 26(3) :618 (in Chinese) [姜岩峰, 黄庆安. 硅各向异性腐蚀的原子级模拟. 半导体学报, 2005, 26(3) :618]
- [11] Zhou Zaifa, Huang Qing'an, Li Weihua, et al. A novel 3-D dynamic cellular automata model for photoresist etching process simulation. IEEE Trans Computer-Aided Design of Integrated Circuits and Systems, accepted
- [12] Ferguson R A. Modeling and simulation of reaction kinetics in advanced resist processes for optical lithography. PhD Dissertation, University of California, Berkeley, 1991
- [13] Yeung S, Derek L, Robert L, et al. Extension of the Hopkins theory of partially coherent imaging to include thin-film interference effects. Proc SPIE, 1993, 1927 :452
- [14] Dill F H, Neureuther A R, Tuttle J A, et al. Modeling projection printing of positive photoresists. IEEE Trans Electron Devices, 1975, 22(2) :456
- [15] Erdmann A, Henke W, Robertson S, et al. Comparison of simulation approaches for chemically amplified resists. Proc SPIE, 2001, 4404 :99
- [16] Roberson S, Mack C A, Maslow M. Towards a universal resist dissolution model for lithography simulation. Proc SPIE, 2001, 4004 :111
- [17] Jakatdar N, Bao J W, Spanos C J, et al. A parameter extraction framework for DUV lithography simulation. Proc SPIE, 1999, 3677 :447
- [18] Baluswamy P, Weatherly A, Kewley D, et al. Practical resist model calibration. Proc SPIE, 2003, 5040 :1556

集成电路和微电子机械系统加工过程中的光刻工艺模拟*

周再发[†] 黄庆安 李伟华

(东南大学 MEMS 教育部重点实验室, 南京 210096)

摘要: 基于 3D 元胞自动机方法实现了影像成形、曝光、后烘和光刻胶刻蚀过程等集成电路和微电子机械系统加工过程中的光刻过程模拟模块的集成. 模拟结果与已有实验结果一致, 表明基于 3D 元胞自动机方法的后烘和光刻胶刻蚀模拟模块的有效性, 这对于实现集成电路和微电子机械系统的器件级的工艺模拟具有一定的实用性.

关键词: 元胞自动机; 工艺模拟; 光刻模拟; 模型; 计算机辅助设计

EEACC: 2570; 2560; 2550E

中图分类号: TN4 **文献标识码:** A **文章编号:** 0253-4177(2006)04-0705-07

* 国家杰出青年科学基金资助项目(批准号:50325519)

[†] 通信作者. Email:zhouzaifa@yahoo.com.cn

2006-01-17 收到, 2006-02-15 定稿